

ORIGINAL ARTICLE

Low-dose endostatin normalizes the structure and function of tumor vasculature and improves the delivery and anti-tumor efficacy of cytotoxic drugs in a lung cancer xenograft murine model

Tao Ning^{1*}, Ming Jiang^{1*}, Qian Peng^{1*}, Xi Yan¹, Ze-Jun Lu¹, Yu-Lan Peng², He-Lan Wang¹, Na Lei¹, Hui Zhang¹, Hong-jun Lin¹, Mei Li¹ & Feng Luo¹

1 Department of Medical Oncology, Cancer Center and State Key Laboratory of Biotherapy, West China Hospital of Sichuan University, Chengdu, Sichuan Province, China

2 Department of Ultrasound, West China Hospital of Sichuan University, Chengdu, Sichuan Province, China

Keywords

endostatin; normalize; tumor vasculature.

Correspondence

Feng Luo, Department of Medical Oncology, Cancer Center and State Key Laboratory of Biotherapy, West China Hospital of Sichuan University, 37 Guoxue Xiang Street, Chengdu 610041, Sichuan Province, China.

Tel: +86 28 8542 2683

Fax: +86 28 8516 4060

Email: luofeng@medmail.com.cn

Received: 30 November 2011;

accepted 4 January 2012.

doi: 10.1111/j.1759-7714.2012.00111.x

*Contributed equally.

Abstract

Introduction: To some extent endostatin normalizes tumor vasculature. However, the optimum time window and optimum drug dose for tumor vascular normalization need to be explored. Here we investigate the effect of low-dose endostatin on the structure and function of tumor vasculature and the delivery and anti-tumor efficacy of cytotoxic drugs.

Methods: A lung cancer xenograft murine model was treated with low-dose endostatin for 10 days. The structure and function of the tumor vasculature were evaluated using various techniques. Paclitaxel was added in different schedules.

Results: Endostatin caused a significant reduction in microvessel density. Tumor vascular walls after endostatin treatment were better structured. Tumor blood perfusion was increased on day six after endostatin administration. On days three, six, and 10, Evans blue extravasation into the parenchyma of tumors was decreased. On days three and six, endostatin-treated mice had greater paclitaxel delivery. The time window of vascular normalization was approximately three to six days. On days one to three, and days four to six, combined therapy with paclitaxel significantly inhibited tumor growth.

Conclusions: Low-dose endostatin aids normalization of tumor vasculature. This resulted in improved delivery of cytotoxic drugs to the tumor, which closely correlates with synergistic efficacy when combined with paclitaxel during the normalization window.

Introduction

The growth and persistence of solid tumors and their metastasis are dependent on angiogenesis.¹⁻³ It is generally acknowledged that inhibition of angiogenesis could be an effective way of controlling tumor development.^{3,4} Many anti-angiogenic agents have been tested pre-clinically and some are undergoing clinical trials.⁵ However, several lines of direct and indirect evidence indicate that these agents have no significant effect on patients with cancer when used alone. However, they have a synergistic effect when administered in combination with chemotherapy.⁶⁻⁸ Research is therefore

required to improve our understanding of the underlying mechanisms of this phenomenon.

Several years ago, Jain⁹ proposed a hypothesis that certain anti-angiogenic agents could transiently normalize the abnormal structure and function of tumor vasculature to make it more efficient for oxygen and drug delivery. These agents can alleviate hypoxia and increase the efficacy of conventional therapies if both are carefully scheduled. Subsequently, it has been found that many compounds that inhibit tumor vascular growth factor pathways (ie vascular endothelial growth factor receptor [VEGFR] and epidermal growth factor receptor [EGFR]) have the ability to normalize the

tumor vasculature.^{10–12} During the normalization window, combining administration of anti-angiogenic agents with chemotherapy or radiotherapy has shown the best synergistic anti-tumor effect.

In theory, any therapy that restores the balance between pro- and anti-angiogenic molecules should induce normalization of the tumor vasculature.^{13,14} Endostatin, a broad-spectrum anti-angiogenic agent, may be a candidate for remodeling the tumor vasculature to a more normal state. Recently, a few preliminary studies investigating this idea have shown that endostatin can improve tumor hypoxia or normalize the tumor vasculature, and thus enhance anti-tumor efficacy when administered in combination with radiotherapy or chemotherapy.^{15–17} These studies have provided a theoretical basis for further research in this field. However, all the studies used a previously designed combined protocol, without investigating the effect of endostatin alone on the tumor vasculature. Thus, we cannot really understand whether the dynamic changes in tumor vasculature, or normalization of tumor vasculature, are due to endostatin treatment in such situations or not, because cytotoxic therapy might also have an effect on anti-angiogenesis and moderate the tumor microenvironment.¹⁸ In addition, higher doses of endostatin were used in these studies, and the structure and function of tumor vasculature were not profoundly explored. Clearly, urgent research into the optimum time window and optimum drug dose for tumor vascular normalization is needed.

Emerging evidence has shown that higher doses of anti-angiogenic agents can compromise the delivery of drugs to tumors and antagonize the outcome of traditional therapy.⁹ Such doses are likely to adversely affect the vasculature of normal tissues. Indeed, anti-angiogenic therapy with agents such as bevacizumab is associated with an increased risk of arterial thromboembolic events, which are more pronounced with increased doses.¹⁹ A recent study has demonstrated that the objective response rate for low-dose bevacizumab in patients with lung cancer is greater than that for high-dose bevacizumab.²⁰ Until now, unfortunately, there has been no information about the effect of low-dose endostatin on normalizing the tumor vasculature. Therefore, in the present study, we first treated tumor-bearing mice with low-dose endostatin for normalization of the tumor vasculature. We then designed an experimental protocol for combining endostatin and cytotoxic drugs to evaluate pharmacokinetic delivery and their probable synergistic anti-tumor effect.

Methods

Cell culture and animal tumor model

The human lung adenocarcinoma cell line SPC-A1 (Chinese Academy of Sciences, Shanghai, China) was maintained in

RPMI-1640 medium supplemented with 10% fetal bovine serum and kept in a humidified five percent CO₂ atmosphere incubator at 37°C. Female athymic nude mice (five to six weeks old) were purchased from the Laboratory Animal Center of Sichuan University (Chengdu, Sichuan, China). A human lung adenocarcinoma xenograft model was established by subcutaneous injection of 3×10^6 SPC-A1 cells into the right dorsal flank of the mice. Calipers were used to measure subcutaneous tumors. Tumor volume was calculated using the following formula: tumor volume (mm³) = width² × length × 0.52. The Animal Care and Use Committee of Sichuan University approved all animal studies.

Histology and immunohistochemistry

When the tumor volume reached approximately 200 mm³, mice were randomized into two groups: one group received a low dose of 3 mg/kg endostatin (recombinant human endostatin; Simcere Medgenn Bio-Pharmaceutical Company, China) daily for 10 days via a tail vein injection; the other group served as control (normal sodium daily for 10 days). Five animals in each group were killed at three different time points (days three, six, and 10). Half of each dissected tumor was fixed in 10% formalin and embedded in paraffin; the other half was snap-frozen and fixed in 3% glutaraldehyde for transmission electron microscopy (TEM). For histology and immunohistochemistry, adjacent sections (thickness, 3–5 μm) were routinely stained with hematoxylin and eosin (H&E). Microvessels were stained with goat anti-mouse CD31 (Santa Cruz, CA, USA) and mural cells were stained with mouse anti-human smooth muscle actin (SMA) antibodies (DAKO, Carpinteria, CA, USA). Microvessel density (MVD) and mural cell density (MCD) were evaluated using methods described previously.¹⁰ In brief, areas with the most microvessels within the tumor were identified. MVD was determined by counting the number of CD31-positive-stained vessels at a magnification of ×400. MCD was obtained by measuring the pixel area of the α-SMA-positive-stained vessels at a magnification of ×400 using Image-Pro Plus 5.1 software. At least three random fields were evaluated for each section, and the average was taken as the MVD or MCD.

Transmission electron microscopy

Glutaraldehyde-fixed tumors were used for TEM. Samples were prepared as described previously.²¹ In brief, the excised tumors were trimmed to a maximal dimension of 1 mm and snap-frozen and fixed with 3% glutaraldehyde for a minimum of two hours and 1% OsO₄ for 30 minutes. Specimens were then removed, dehydrated with acetone, and embedded in epoxy resin. For light microscopy, 1-μm-thick sections were stained with toluidine blue, and 70-nm-thick sections were stained with lead citrate and uranyl acetate.

Then the intratumoral vasculature was visualized using an H7650 transmission electron microscope (Japan).

Contrast-enhanced ultrasonography

To study the modulation of tumor vasculature by endostatin further, another set of SPC-A1 tumor-bearing mice was used. Five animals in each group at three different time points (days three, six, and 10) underwent contrast-enhanced ultrasonography using a Philips iU22 L9-3 ultrasound machine, according to a method described previously with some modifications.²² The machine's mechanical index was adjusted to <0.1 to prevent microbubble destruction. Sono Vue (Bracco, Italy) was used as the contrast agent. In brief, mice bearing SPC-A1 xenografts were anesthetized and received a bolus injection into a tail vein of 0.1 mL of microbubble contrast agent diluted in 0.1 mL of saline. Immediately after injection of the contrast agent, images were recorded on cine clips at a frame rate of 10–40 Hz for 60 seconds. The clips were later analyzed online using Q-LAB software.

Vascular permeability and hemorrhage assay

After contrast-enhanced ultrasonography, animals were tested for vessel permeability using an Evans blue dye method, as described previously.¹¹ Briefly, 100 μ L of 2% Evans blue dye (Sigma, USA) was injected intravenously and allowed to circulate for 20 minutes. Thereafter the mice were killed. Tumors were excised and weighed before Evans blue extraction in 1 mL of formamide for 72 hours. Levels of the dye were then quantified using a spectrophotometer at a wavelength of 620 nm. Hemorrhage inside the tumors was assessed using sections stained with H&E.

Intratumoral drug delivery

Another set of SPC-A1 tumor-bearing mice was used for the evaluation of cytotoxic drug delivery. On days three, six, and 10 after endostatin treatment, animals received a bolus injection of 10 mg/kg paclitaxel into the tail vein ($n = 5$ animals/group at each time point). The concentration of paclitaxel in animal plasma and in tumor tissue was evaluated using a reversed-phase high-performance liquid chromatographic (HPLC) method, as reported previously.²³ One hour after this injection, whole blood (in EDTA) and tumor tissues were collected for analysis. Tumors were homogenized in phosphate-buffered saline (5 mL/mg tissue). Plasma was collected from the whole blood. Docetaxel was routinely used as an internal standard. The tissue homogenates (500 mL) and plasma (100 mL) containing docetaxel were then extracted using 500 mL of methanol and 2 mL of ethyl acetate, respectively. Chromatographic separation was carried out with a Waters

2695–2996 SunFire C18 reversed-phase column (4.6×150 mm, 5 μ m) at $25 \pm 5^\circ\text{C}$. The mobile phase consisted of HPLC-grade acetonitrile and 35 mM ammonium acetate buffer (pH 5.0), with acetonitrile linear gradients from 30% to 70% acetonitrile in 10 minutes, then a linear gradient to 30% acetonitrile in 12 minutes; this was delivered at a flow rate of 1 mL/minute. Ultraviolet detection was performed at 230 nm.

Treatment protocol

SPC-A1 human lung adenocarcinoma xenografts were again established as described above. When the tumor volume reached about 200 mm³, animals were divided into six groups ($n = 7$ animals/group): group 1 served as normal saline group (NS); group 2 received 10 mg/kg paclitaxel intravenously daily for three days (PT); group 3 received 3 mg/kg endostatin intravenously daily for 10 days (ES). On days one to three, four to six, and eight to 10 after the initiation of endostatin treatment (group 3), 10 mg/kg paclitaxel was combined intravenously daily and these groups were defined as group 4 (combined 1), group 5 (combined 2), and group 6 (combined 3), respectively. All animals were killed on day 15 and tumor size was assessed. Animals were also observed for possible side effects during the treatment.

Statistical analysis

SPSS 13.0 was used to analyze the data. Differences between groups were tested by analysis of variance and an unpaired Student's *t*-test. A *P*-value <0.05 was considered statistically significant.

Results

Endostatin decreases MVD without affecting MCD

We first examined the effect of low-dose endostatin on MVD and MCD in mice bearing SPC-A1 xenografts. On days three, six, and 10 after endostatin administration, the MVD was reduced to 84.8%, 72.9% and 67.2%, respectively. There was a significant difference in the MVD between the endostatin and the control groups on days six and 10 ($P < 0.05$; Fig 1a,b). However, no significant difference in the α -SMA density between the endostatin and the control groups was observed ($P > 0.05$; Fig 1a,c). These results suggest that low-dose endostatin induces regression of endothelial cells without a corresponding loss of mural cells. Under light microscopy, CD31-stained sections showed that microvessels within control tumors were chaotic with abrupt changes in vessel direction, whereas microvessels in endostatin-treated tumors were more regularly distributed and had fewer giant

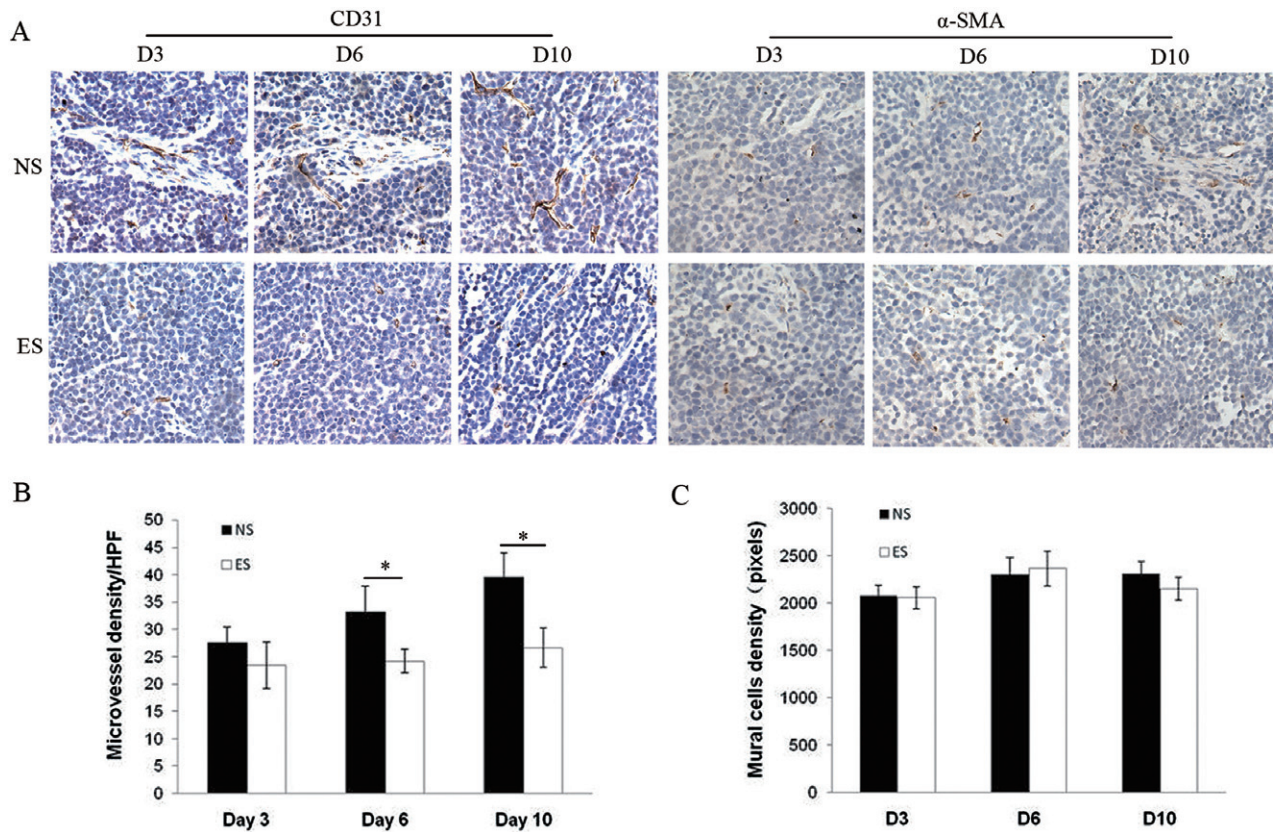


Figure 1 Immunohistologic evaluation of the effect of low-dose endostatin on the intratumoral vasculature. (a) Representative CD31 and α -smooth muscle actin (α -SMA) immunohistochemistry on days three, six, and ten. Original magnification: $\times 400$. (b) Immunohistochemistry analysis of microvessel density (MVD). (c) Quantitative comparison of α -SMA-positive area in tumor sections between the endostatin-treated (ES) and normal control (NS) groups. Data is shown as mean \pm SD. Columns, means; bars, SD; * $P < 0.05$.

branches. Thus, we propose that endostatin may have re-modeled the tumor vasculature.

Endostatin normalizes architecture of the tumor vascular wall

Architecture alterations of the tumor vascular walls after endostatin treatment were examined further using TEM to visualize the intratumoral vessels. We found that the structure of the tumor vascular walls in the control groups was chaotic. Basement membranes were loosely associated with endothelial cells and in some regions extended away from the vessel wall. Some regions of the vascular basement membrane were multilayered. In addition, pericytes in the control tumors were abnormally shaped (Fig 2a,b). During the process of vessel regression induced by endostatin, the surviving vessels had a more normal vascular wall structure (Fig 2c,d). These findings suggest that low-dose endostatin resulted in maturation of the tumor vascular wall and provided the intratumoral vessels with a more “normalized” morphologic phenotype.

Endostatin reduces intratumoral hemorrhage and tumor vessel leakiness

Tumor vessels lack the tight endothelial monolayer essential for normal barrier function, and this results in leakiness and hemorrhage. So intratumoral vascular hemorrhage and permeability were also evaluated after endostatin treatment. We found that tumors in the control groups were very bloody compared with those in the endostatin-treated groups. A large amount of erythrocytes extravasated from the tumor vessels and contributed to blood pools in the tumor mesenchyma. However, an obvious reduction in the blood pools was seen inside the tumors after endostatin treatment (Fig 3a). We then examined whether endostatin might affect vessel leakiness inside the tumors, using sections stained with H&E. We found that endostatin induced a significant reduction in tumor vessel permeability. On days three, six, and 10 after the administration of endostatin, Evans blue dye extravasating into the parenchyma of tumors decreased to 96.1% ($123.89 \pm 10.00 \mu\text{g/g}$ vs. $119.02 \pm 5.06 \mu\text{g/g}$, $P > 0.05$), 87.6% ($131.89 \pm 7.81 \mu\text{g/g}$ vs. $115.52 \pm 7.70 \mu\text{g/g}$, $P < 0.05$),

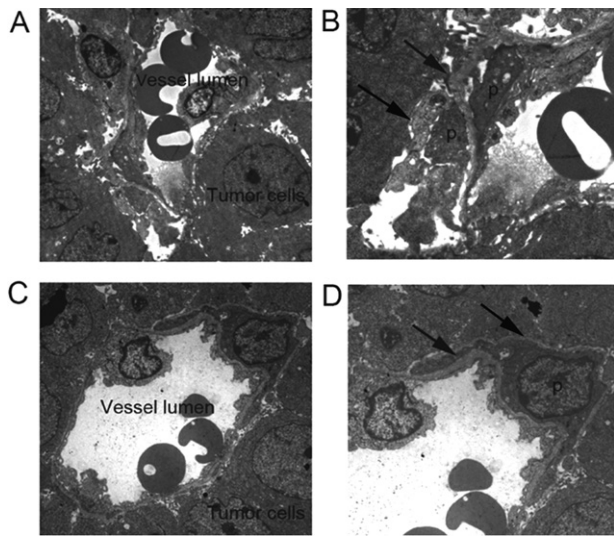


Figure 2 Endostatin normalizes architecture of intratumoral vascular walls. Images shown represent tumors from mice killed on day six. (a) and (b) represent tumors from the control group. (c) and (d) represent tumors from the endostatin-treated group. Original magnification for a and c, $\times 0.7k$; Original magnification for b and d, $\times 1.5k$; P, pericytes or pericyte processes; Arrows, basement membrane.

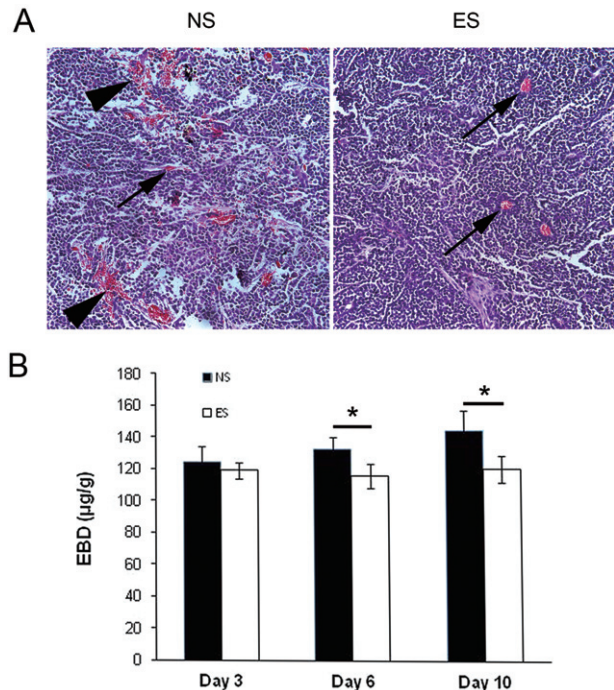


Figure 3 Endostatin alters tumor vascular permeability and hemorrhage. (a) Representative hematoxylin and eosin (H&E) sections at day six. Original magnification: $\times 200$. Long thin arrows, blood vessels; short arrows, blood pools. (b) Vessel permeability assessed by Evans blue dye (EBD). Data is shown as mean \pm SD. Columns, means; bars, SD. * $P < 0.05$.

and 83.5% ($143.67 \pm 12.74 \mu\text{g/g}$ vs. $119.97 \pm 8.42 \mu\text{g/g}$, $P < 0.05$), respectively (Fig 3b). These results suggest that low-dose endostatin promoted some degree of normalization in the tumor vasculature.

Endostatin transiently increases tumor blood perfusion

We then evaluated whether these alterations in the tumor vessels affected tumor blood perfusion using quantitative contrast-enhanced ultrasonography. Tumor-bearing mice received an intravenous injection of ultrasound contrast agent, and then intratumoral blood perfusion was assessed by the changes in signal intensity (ΔSI in decibels), as reported previously.²² As shown in Figure 4a, contrast enhancement in the endostatin-treated mice was more homogeneous throughout the tumor mass, but mainly restricted to the periphery in the control mice. On day six after endostatin treatment, the ΔSI increased by 24.1% compared with its control ($P < 0.05$). On day three or day 10, no significant difference in the ΔSI was found between the endostatin and control groups ($P > 0.05$; Fig 4b). These results suggest that low-dose endostatin treatment transiently increased tumor blood perfusion.

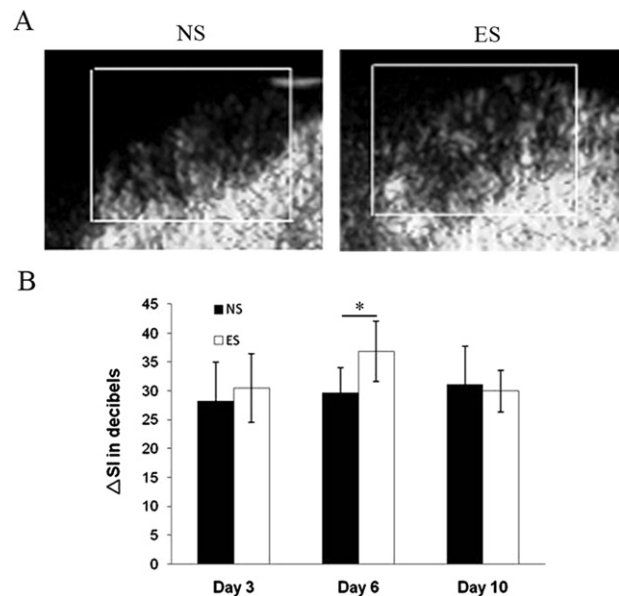


Figure 4 Endostatin transiently increases blood perfusion. (a) Representative contrast-enhanced ultrasound images of normal saline (NS) and endostatin (ES)-treated tumors after intravenous injection of contrast agent on day six. The box shows the subcutaneous tumor. (b) Quantitative comparison of contrast enhancement using Q-LAB analysis software. ΔSI , change in signal intensity. Data is shown as mean \pm SD. Columns, means; bars, SD. * $P < 0.05$.

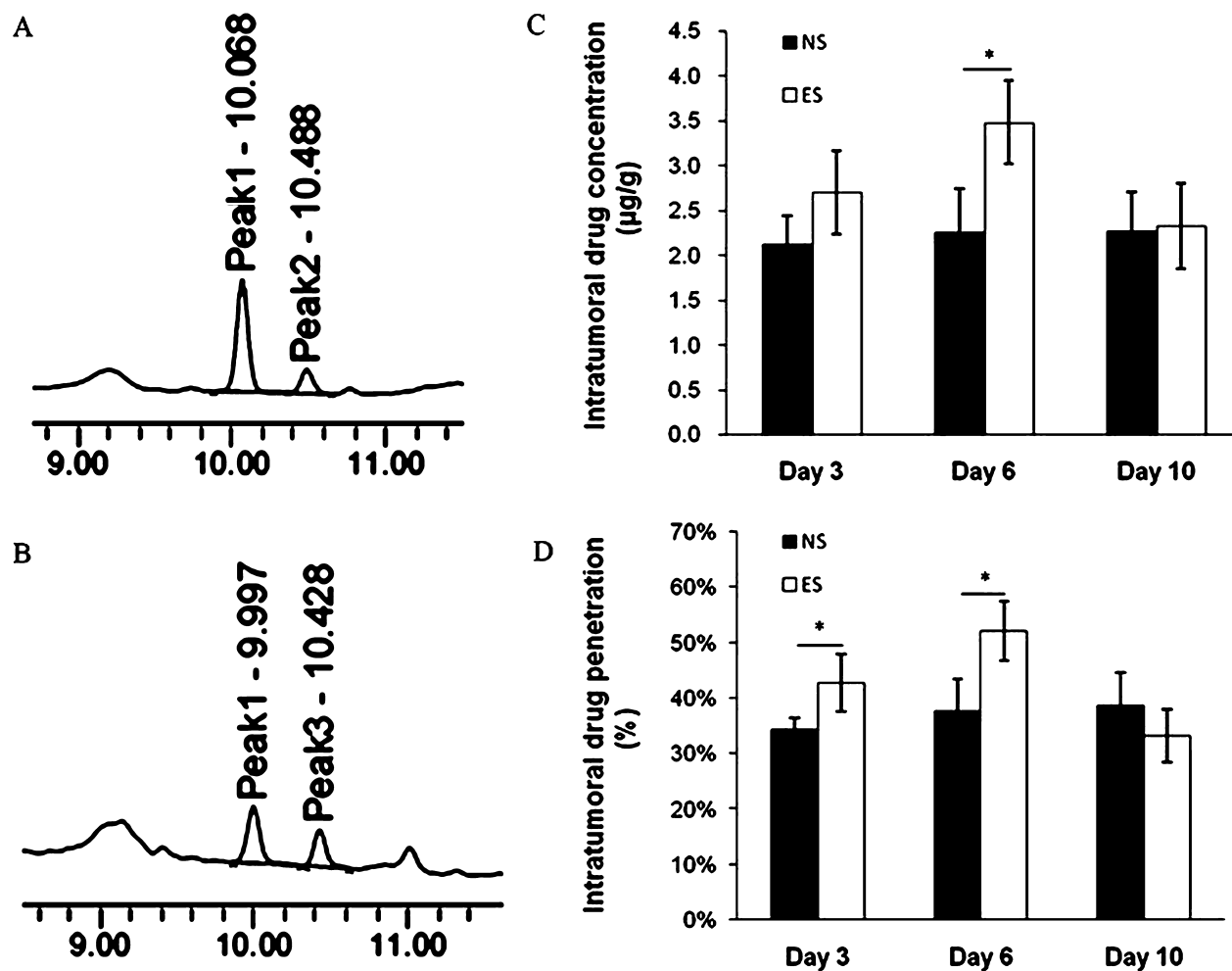


Figure 5 Effect of endostatin on intratumoral drug delivery. Chromatograms of an extracted plasma sample (a) and extracted tumor sample (b). Peak 1, internal standard (docetaxel); peak 2, paclitaxel in the plasma sample; peak 3, paclitaxel in the tumor sample. (c) High-performance liquid chromatography (HPLC) analysis of paclitaxel concentration in the tumors. (d) HPLC analysis of paclitaxel delivery. Data is shown as mean \pm SD. Columns, means; bars, SD. * $P < 0.05$.

Endostatin enhances intratumoral drug delivery

We next tested whether the alterations in the tumor vessel structure and function would improve the efficacy of intratumoral cytotoxic drug delivery. Tumor-bearing mice received a single intravenous injection of 10 mg/kg paclitaxel. Intratumoral and plasma concentrations of paclitaxel were detected using HPLC (Fig 5a,b). As shown in Figure 5c, endostatin treatment produced a trend towards higher intratumoral availability of paclitaxel on day six ($3.48 \pm 0.47 \mu\text{g/g}$ vs. $2.26 \pm 0.49 \mu\text{g/g}$, $P < 0.05$). No significant difference in the mean plasma paclitaxel level was seen between the endostatin and control groups. We also determined the ratio of paclitaxel concentration in the tumor to that in the plasma, as described previously.²⁴ As shown in Figure 5d, endostatin-treated mice

had a higher level of paclitaxel delivery on day three (42.8% vs. 34.3%, $P < 0.05$) and on day six (52.1% vs. 37.7%, $P < 0.05$) than the controls. However, this improvement in drug delivery did not occur on day 10 (33.1% vs. 38.7%, $P > 0.05$). This data suggests that endostatin induced a transient enhancement of drug delivery to the tumor.

Endostatin improves anti-tumor efficacy of paclitaxel

From the data above, we found that low-dose endostatin can normalize the structure and function of the tumor vasculature. The time window of tumor vascular normalization was about three to six days after endostatin administration. Based on this finding, we designed an experimental protocol as described in "Methods." We found that monotherapy with

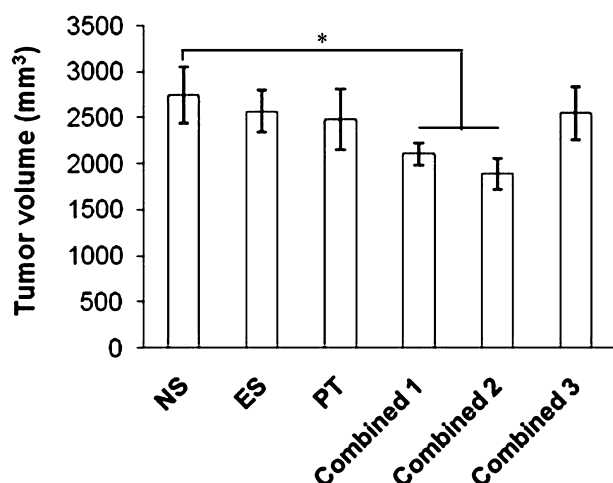


Figure 6 Effect of scheduling administration of paclitaxel in combination with endostatin on tumor growth. Combined 1, paclitaxel was combined on days one to three after the initiation of endostatin treatment; combined 2, paclitaxel was combined on days four to six after the initiation of endostatin treatment; combined 3, paclitaxel was combined on days eight to 10 after the initiation of endostatin treatment. Data is shown as mean \pm SD. Columns, means; bars, SD. * $P < 0.05$. NS, normal saline; ES, endostatin, PT, paclitaxel.

either endostatin or paclitaxel had a minor effect on tumor inhibition compared with that in the control group ($2567.38 \pm 227.03 \text{ mm}^3$ or $2485.34 \pm 329.26 \text{ mm}^3$ vs. $2746.03 \pm 304.66 \text{ mm}^3$; $P > 0.05$; Fig 6). On days one to three, or four to six, after endostatin treatment, addition of paclitaxel significantly inhibited the tumor growth ($2104.01 \pm 121.49 \text{ mm}^3$ or $1890.62 \pm 116.93 \text{ mm}^3$, respectively; $P < 0.05$). However, combined group 2 had an even more pronounced synergistic effect than combined group 1, although the difference did not reach statistical significance. No synergistic effect was found in combined group 3 (2549.66 ± 287.30 ; $P > 0.05$). Treated mice were investigated for potential side effects. No severe adverse consequences were indicated in gross measures. Furthermore, no pathological changes in kidney, brain, heart, or arteries were found by microscopic examination (data not shown).

Discussion

In this study, we used low-dose endostatin to examine the efficacy of normalization of tumor vasculature. We obtained a number of results for tumor vascular changes due to endostatin treatment, combination scheduling, and synergistic efficacy. Low-dose endostatin normalized the structure and function of the tumor vasculature. Different combination scheduling of endostatin with a cytotoxic drug resulted in changed anti-tumor efficacy. The therapeutic synergy of endostatin combined with chemotherapy was thought to be

due to the enhancement of cytotoxic drug delivery into the tumor. Our results support these suggestions. In the lung cancer xenograft murine model, low-dose endostatin induced a significant reduction of MVD, vessel permeability, and hemorrhage within the tumor. The architecture of tumor vascular walls became more organized. Blood perfusion and intratumoral paclitaxel delivery were improved. Endostatin transiently remodeled the structure and function of the tumor vasculature, reaching some degree of normalization, with a time window of three to six days. During this short period of time, the combined endostatin and paclitaxel treatment led to even more pronounced synergistic anti-tumor activity.

In normal tissues, the balance between pro-angiogenic and anti-angiogenic factors maintains the normal structure of the vasculature.⁹ In tumor tissues, tumor vessels grow in circumstances where the balance is tipped towards the pro-angiogenic side. Such vessels are abnormal in structure and function.^{13,14} The view held is that tumor vasculature could be normalized by certain anti-angiogenic agents.⁹ Recent studies using anti-angiogenic agents such as bevacizumab, sunitinib, or erlotinib have shown that in addition to their potent effects on MVD inhibition, these agents also alter the morphology and function of the tumor vasculature, thus altering the tumor microenvironment and affecting the efficacy of chemotherapy or radiotherapy.^{10–12}

Endostatin, a specific endogenous anti-angiogenic factor, might be a candidate for remodeling of the tumor vasculature. Recently, several studies have reported their results about endostatin on this issue. Wen *et al.*¹⁷ found that endostatin significantly sensitizes radiation function in anti-tumor efficacy and anti-angiogenesis by increasing apoptosis of endothelial cells and tumor cells, improving hypoxia of tumor cells, and changing pro-angiogenic factors. Jiang *et al.*¹⁵ also found that radiotherapy combined with endostatin could significantly inhibit tumor growth and induce earlier tumor regression, which may be related to the improvement of tumor hypoxia and the inhibition of radiation-induced tumor angiogenesis. However, in both of these studies the combined protocol had been designed before proceeding to investigate the effect of endostatin on the tumor microenvironment. Actually, radiotherapy also has an effect on anti-angiogenesis and moderates the tumor microenvironment.¹⁸ In addition, Huang *et al.*¹⁶ reported the effect of endostatin on the normalization of tumor vasculature. They had also designed the combined protocol before proceeding to investigate the effect of endostatin alone on the structure and function of tumor vasculature. According to Jain's hypothesis, tumor vascular normalization remodeled by anti-angiogenic agents should have an optimal time window. During this time window, anti-angiogenic agents, when given in combination with chemotherapy, can obtain the best synergistic anti-tumor activity.^{9,13}

In the present study, we first treated tumor-bearing mice with low-dose endostatin alone for normalization of tumor vasculature. We found that endostatin significantly reduced tumor MVD but had no effect on MCD, indicating that endostatin induces endothelial cell regression without a corresponding loss of mural cells. Mural cells are key components in vascular development, stabilization, maturation, and remodeling. Absence of mural cells is attributed to the vulnerability of newly formed blood vessels.²⁵ So, we speculate that endostatin can selectively prune some immature newly formed microvessels and transform others into a more normal phenotype. Our findings are consistent with a previous report in which tumors in endostatin-treated mice displayed fewer, less tortuous, branched vessels, resembling a granulation tissue-like microvasculature.²⁶

Abnormal tumor vasculature results in an abnormal tumor microenvironment, and together they pose a formidable barrier to effective drug delivery and effective cancer therapy.²⁷ In our study, we also found that endostatin caused a functional alteration of the tumor vasculature. It induced an obvious reduction in tumor vascular permeability and hemorrhage, whereas tumor blood perfusion and intratumoral drug delivery were transiently improved. In previous studies, tumor drug delivery has usually been investigated by determining the intratumoral concentration of drugs using HPLC.^{28,29} However, this method did not consider the distribution of drugs in the blood circulation. In the present study, in addition to detecting the intratumoral concentration of paclitaxel, we also used the method described by Dickson *et al.*²⁴ in which drug delivery was determined as the ratio of paclitaxel concentration in the tumor to that in the plasma, thus taking into account intratumoral drug penetration and fluctuations in plasma paclitaxel concentration. We found that endostatin-treated mice had a higher level of paclitaxel delivery on days three and six, and that endostatin improved tumor penetration of systemically administered cytotoxic drugs.

The dose of anti-angiogenic agents is important for anti-tumor activity.⁹ It is tempting to increase the doses of anti-angiogenic agents to obtain greater efficacy. However, excessive vascular regression by anti-angiogenic agents may be counterproductive because it compromises the delivery of drugs and oxygen.¹³ Furthermore, increased doses of currently available anti-angiogenic therapies are likely to adversely affect the vasculature of normal tissues, including the cardiovascular, urinary, and nervous systems.⁹ Indeed, anti-angiogenic therapy with agents such as bevacizumab is associated with an increased risk of arterial thromboembolic events, hypertension, and proteinuria.^{19,30} Studies evaluating the safety and efficacy of bevacizumab in patients with breast cancer also found that higher doses of bevacizumab increased toxicity but did not result in significant survival benefit.³¹ In the previously mentioned studies, higher doses of endostatin

were administered. Wen *et al.* used endostatin at a dose of 20 mg/kg once daily for 10 days.¹⁷ Huang *et al.*¹⁶ gave mice a dose of 5 mg/kg endostatin for seven days, and Jiang *et al.*¹⁵ treated mice with 0.2 mL of endostatin (0.75 mg/mL) for seven days. In our study, we chose a low dose of endostatin (3 mg/kg daily for 10 days) and found that low-dose endostatin normalized the structure and function of the tumor vasculature. During the vasculature normalization period, the combination of endostatin and paclitaxel resulted in the best synergistic anti-tumor activity, with no severe adverse consequences.

In our study, we found that endostatin transiently remodeled the structure and function of the tumor vasculature. During a short period of time, the combination of endostatin and paclitaxel treatment led to even more pronounced synergistic anti-tumor activity. Our findings are consistent with those from other studies in which anti-angiogenic therapy with DC101³² or bevacizumab²⁴ could also transiently remodel the tumor vasculature. What is the reason for this phenomenon? Tumor vasculature is structurally and functionally abnormal. Actually, anti-angiogenic therapies can initially improve both the structure and function of tumor vessels. However, sustained or aggressive anti-angiogenic regimens may eventually prune away these vessels, resulting in a vasculature that is inadequate for the delivery of drugs or oxygen.⁹

However, there are some weaknesses in our study. First, as collecting tumor specimens for detecting MVD, MCD, and Evans blue dye (EBD) is invasive, we had to kill animals at different time points. Therefore, we had no chance of continuous and dynamic monitoring of changes in the tumor vasculature after endostatin administration. Second, interstitial fluid pressure and microvessel pressure, which served as useful indicators for tumor vessel function, have not been evaluated due to equipment limitations in our laboratory. Finally, tumor blood perfusion was initially shown by contrast-enhanced ultrasonography. More advanced technology that can provide more detailed parameters, such as vascular volume, blood perfusion, and uptake of some drugs, is therefore needed to monitor the tumor vascular status in the future.

Conclusion

In conclusion, we have shown that low-dose endostatin produces transient normalization of tumor vasculature in mice bearing human lung cancer xenografts. Remodeling of the tumor vasculature resulted in improved delivery of the cytotoxic drug into the tumor. The improved delivery correlated closely with synergistic efficacy when endostatin was combined with paclitaxel. As anti-angiogenic agents continue to be studied in clinical trials, optimal scheduling of anti-angiogenic therapy combined with chemotherapy requires a

deep understanding of the molecular mechanisms and the associated pharmacokinetic and pharmacodynamic variables for this combination therapy. Our observations may provide a rational basis for future research into the application and improvement of this combination strategy.

Acknowledgment

The National Science Foundation of China supported this research (No. 30972971, No. 81071864).

Disclosure

No authors report any conflict of interest.

References

- Folkman J. Angiogenesis. *Annu Rev Med* 2006; **57**: 1–18.
- Hashizume H, Falcon BL, Kuroda T *et al.* Complementary actions of inhibitors of angiopoietin-2 and VEGF on tumor angiogenesis and growth. *Cancer Res* 2010; **70**: 2213–23.
- Chakroborty D, Sarkar C, Basu B, Dasgupta PS, Basu S. Catecholamines regulate tumor angiogenesis. *Cancer Res* 2009; **69**: 3727–30.
- Gordon MS, Mendelson DS, Kato G. Tumor angiogenesis and novel antiangiogenic strategies. *Int J Cancer* 2010; **126**: 1777–87.
- Damia G, D'Incalci M. Contemporary pre-clinical development of anticancer agents – what are the optimal preclinical models? *Eur J Cancer* 2009; **45**: 2768–81.
- Gasparini G, Longo R, Fanelli M, Teicher BA. Combination of antiangiogenic therapy with other anticancer therapies: results, challenges, and open questions. *J Clin Oncol* 2005; **23**: 1295–311.
- Welch S, Spithoff K, Rumble RB, Maroun J, Gastrointestinal Cancer Disease Site Group. Bevacizumab combined with chemotherapy for patients with advanced colorectal cancer: a systematic review. *Ann Oncol* 2010; **21**: 1152–62.
- Ning T, Yan X, Lu ZJ *et al.* Gene therapy with the angiogenesis inhibitor endostatin in an orthotopic lung cancer murine model. *Hum Gene Ther* 2009; **20**: 103–11.
- Jain RK. Normalization of tumor vasculature: an emerging concept in antiangiogenic therapy. *Science* 2005; **307**: 58–62.
- Zhou Q, Guo P, Gallo JM. Impact of angiogenesis inhibition by sunitinib on tumor distribution of temozolomide. *Clin Cancer Res* 2008; **14**: 1540–9.
- Cerniglia GJ, Pore N, Tsai JH *et al.* Epidermal growth factor receptor inhibition modulates the microenvironment by vascular normalization to improve chemotherapy and radiotherapy efficacy. *PLoS ONE* 2009; **4**: 1–11.
- Myers AL, Williams RF, Ng CY, Hartwich JE, Davidoff AM. Bevacizumab-induced tumor vessel remodeling in rhabdomyosarcoma xenografts increases the effectiveness of adjuvant ionizing radiation. *J Pediatr Surg* 2010; **45**: 1080–5.
- Jain RK. A new target for tumor therapy. *N Engl J Med* 2009; **360**: 2669–71.
- De Bock KD, Cauwenberghs S, Carmeliet P. Vessel abnormalization: another hallmark of cancer? Molecular mechanisms and therapeutic implications. *Curr Opin Genet Dev* 2011; **21**: 73–9.
- Jiang XD, Dai P, Wu J, Song DA, Yu JM. Inhibitory effect of radiotherapy combined with weekly recombinant human endostatin on the human pulmonary adenocarcinoma A549 xenografts in nude mice. *Lung Cancer* 2011; **72**: 165–71.
- Huang G, Chen L. Recombinant human endostatin improves anti-tumor efficacy of paclitaxel by normalizing tumor vasculature in Lewis lung carcinoma. *J Cancer Res* 2010; **136**: 1201–11.
- Wen QL, Meng MB, Yang B *et al.* Endostar, a recombinant humanized endostatin, enhances the radioresponse for human nasopharyngeal carcinoma and human lung adenocarcinoma xenografts in mice. *Cancer Sci* 2009; **100**: 1510–19.
- Kerbel RS, Emmenegger U, Man S, Munoz R, Folkins C, Shaked Y. Metronomic low-dose antiangiogenic chemotherapy in mice and man. *Nat Rev Cancer* 2004; **4**: 423–36.
- Ratner M. Genentech discloses safety concerns over Avastin. *Nat Biotechnol* 2004; **22**: 1198.
- Reck M, von Pawel J, Zatloukal P *et al.* Phase III trial of cisplatin plus gemcitabine with either placebo or bevacizumab as first-line therapy for nonsquamous non-small-cell lung cancer: AVAIL. *J Clin Oncol* 2009; **27**: 1227–34.
- Inai T, Mancuso M, Hashizume H *et al.* Inhibition of vascular endothelial growth factor (VEGF) signaling in cancer causes loss of endothelial fenestrations, regression of tumor vessels, and appearance of basement membrane ghosts. *Am J Pathol* 2004; **165**: 35–52.
- Quaia E. Assessment of tissue perfusion by contrast-enhanced ultrasound. *Eur Radiol* 2011; **21**: 604–15.
- Kim SC, Yu J, Lee JW, Park ES, Chi SC. Sensitive HPLC method for quantitation of paclitaxel (Genexol) in biological samples with application to preclinical pharmacokinetics and biodistribution. *J Pharmaceut Biomed Anal* 2005; **39**: 170–6.
- Dickson PV, Hamner JB, Sims TL *et al.* Bevacizumab-induced transient remodeling of the vasculature in neuroblastoma xenografts results in improved delivery and efficacy of systemically administered chemotherapy. *Clin Cancer Res* 2007; **13**: 3942–50.
- Baluk P, Hashizume H, McDonald DM. Cellular abnormalities of blood vessels as targets in cancer. *Curr Opin Genet Dev* 2005; **15**: 102–11.
- Read TA, Farhadi M, Bjerkvig R *et al.* Intravital microscopy reveals novel antivascular and antitumor effects of endostatin delivered locally by alginate-encapsulated cells. *Cancer Res* 2001; **61**: 6830–7.
- Goel S, Duda DG, Xu L, *et al.* Normalization of the vasculature for treatment of cancer and other diseases. *Physiol Rev* 2011; **91**: 1071–121.

- 28 Wildiers H, Guetens G, De Boeck G *et al.* Effect of anti-vascular endothelial growth factor treatment on the intratumoral uptake of CPT-II. *Br J Cancer* 2003; **88**: 1979–86.
- 29 Bhattacharya A, Seshadri M, Oven SD, Tóth K, Vaughan MM, Rustum YM. Tumor vascular maturation and improved drug delivery induced by methylselenocysteine leads to therapeutic synergy with anticancer drugs. *Clin Cancer Res* 2008; **14**: 3926–32.
- 30 Yang JC, Haworth L, Sherry RM *et al.* A randomized trial of bevacizumab, an anti-vascular endothelial growth factor antibody, for metastatic renal cancer. *N Engl J Med* 2003; **349**: 427–34.
- 31 Cobleigh MA, Langmuir VK, Sledge GW *et al.* A phase I/II dose-escalation trial of bevacizumab in previously treated metastatic breast cancer. *Semin Oncol* 2003; **30** (Suppl.): 117–24.
- 32 Tong RT, Boucher Y, Kozin SV, Winkler F, Hicklin DJ, Jain RK. Vascular normalization by vascular endothelial growth factor receptor 2 blockade induces a pressure gradient across the vasculature and improves drug penetration in tumors. *Cancer Res* 2004; **64**: 3731–6.